

CAN THE SUPER-KAMIOKANDE ATMOSPHERIC DATA PREDICT THE SOLAR NEUTRINO DEFICIT ?

ION STANCU*

*Department of Physics, University of California
 Riverside, CA 92521, USA*

Received 29 March 1999

Revised 31 March 1999

In this Letter we show that the evidence for neutrino oscillations from the Super-Kamiokande atmospheric neutrino data fully determines the 3×3 neutrino-oscillations mixing matrix and predicts an energy independent solar neutrino deficit at the level of 45%. This corresponds to a ratio of measured to predicted neutrino flux of $R_e^{Solar} = 0.55$, in good agreement with the experimental results. We achieve this result within the framework of a minimal, three-generations neutrino mixing, with mass squared differences of $\Delta M^2 \simeq 0.45 \text{ eV}^2$ and $\Delta m^2 = \mathcal{O}(10^{-3}) \text{ eV}^2$. The mixing matrix derived here is characterized by the mixing angles $\theta = 35.1^\circ$, $\beta = 5.5^\circ$, and $\psi = 23.3^\circ$, and a vanishing CP-violating phase, $\delta = 0$.

Keywords: Neutrino oscillations

1. Introduction

The phenomenon of neutrino oscillations was first postulated by Pontecorvo¹ in 1957, and has been ever since a prime candidate in explaining the long-standing puzzle provided by the solar neutrino deficit.^{2,3,4,5,6} The anomalies reported in the atmospheric neutrino production^{7,8,9} and the positive signals obtained by LSND in both the $\bar{\nu}_\mu \rightarrow \bar{\nu}_e$ and the $\nu_\mu \rightarrow \nu_e$ appearance channels^{10,11} have contributed to further strengthen the evidence towards neutrino oscillations. At the same time, these observations raise the question whether they can all be explained in the minimal, three-generation neutrino mixing formalism. Typically, all experiments have been analyzed in terms of the simpler, two-neutrino oscillation hypothesis, which in turn have given rise to three different mass squared differences, δm^2 . The solar neutrino deficit implies a δm^2 of $\mathcal{O}(10^{-10}) \text{ eV}^2$ or $\mathcal{O}(10^{-5}) \text{ eV}^2$, corresponding to vacuum or MSW oscillations, respectively. The atmospheric neutrino deficit indicates a δm^2 of $\mathcal{O}(10^{-3}) \text{ eV}^2$. The LSND evidence points towards a δm^2 of $\mathcal{O}(1) \text{ eV}^2$. Since only two mass squared differences are independent, one possible solution to this puzzle is the introduction of a fourth neutrino flavor, which must be sterile if its mass is low. Another solution is to ignore one of the indications listed above, typically LSND, as it is the only evidence that has not been independently confirmed by another ex-

*E-mail: ion.stancu@ucr.edu

periment. (However, one should keep in mind that the LSND evidence comes from two different channels, with different neutrino fluxes, signatures, backgrounds and systematics.) On the other hand, if one assumes that the LSND excess is indeed due to neutrino oscillations, the two mass squared differences implied by it and by the Super-Kamiokande atmospheric data would necessarily lead to an energy independent oscillation probability for the solar neutrinos.

The latter approach has been followed by several authors.^{12,13,14} Using three data points, (1) a flat solar neutrino ratio of $R_e^{Solar} = 0.5$, (2) the atmospheric ν_μ deficit for up-going muons (interpreted as $\nu_\mu \rightarrow \nu_\tau$ oscillations), and (3) the oscillation probability reported by LSND, they fully determine the neutrino-mixing matrix. This, together with the LSND and Super-Kamiokande mass squared differences, is shown to be consistent with all current neutrino oscillations experiments. Alternatively, a more elaborate fit to all data,¹⁵ yields similar results. What we show in this Letter is that the Super-Kamiokande atmospheric data alone contains enough information, through its explicit L/E dependence, to fully determine the neutrino-oscillations mixing matrix, and is able to predict the solar neutrino deficit to a level which is consistent with the current measurements.

2. Formalism

Throughout this paper we shall assume that the three neutrino weak eigenstates (ν_e, ν_μ, ν_τ) are linear superpositions of three mass eigenstates (ν_1, ν_2, ν_3),

$$|\nu_\ell\rangle = \sum_{j=1}^3 U_{\ell j} |\nu_j\rangle \quad (\ell = e, \mu, \tau), \quad (1)$$

with masses $m_1 < m_2 < m_3$. The unitary matrix U , parameterized in terms of three mixing angles (θ, β, ψ) and a CP-violating phase (δ), reads

$$U = \begin{pmatrix} c_\theta c_\beta & s_\theta c_\beta & s_\beta \\ -c_\theta s_\beta s_\psi e^{i\delta} - s_\theta c_\psi & c_\theta c_\psi - e^{i\delta} s_\theta s_\beta s_\psi & c_\beta s_\psi e^{i\delta} \\ -c_\theta s_\beta c_\psi + s_\theta s_\psi e^{-i\delta} & -s_\theta s_\beta c_\psi - c_\theta s_\psi e^{-i\delta} & c_\beta c_\psi \end{pmatrix} \quad (2)$$

in the Maiani representation,¹⁶ where $c_\theta = \cos\theta$, $s_\theta = \sin\theta$, etc. Consequently, assuming that the mass eigenstates are relativistic¹⁷ and stable, the oscillation probability from a state $|\nu_\ell\rangle$ to a state $|\nu_{\ell'}\rangle$ is given by

$$P(\nu_\ell \rightarrow \nu_{\ell'}) = \delta_{\ell\ell'} - \sum_{i=1}^2 \sum_{j=i+1}^3 \left[4 \operatorname{Re}(U_{\ell'i} U_{\ell i}^* U_{\ell'j}^* U_{\ell j}) \sin^2 \left(1.27 \Delta m_{ij}^2 \frac{L}{E} \right) - 2 \operatorname{Im}(U_{\ell'i} U_{\ell i}^* U_{\ell'j}^* U_{\ell j}) \sin \left(2.54 \Delta m_{ij}^2 \frac{L}{E} \right) \right]. \quad (3)$$

In Eq.(3) above E is the neutrino energy (expressed in MeV), L is the distance between the generation point and the detection point (expressed in m), and $\Delta m_{ij}^2 \equiv m_i^2 - m_j^2$ (expressed in eV²). The neutrino mass spectrum is characterized by two

mass squared differences, which we shall loosely refer to as “mass scales” henceforth, Δm^2 and ΔM^2 :

$$\Delta m^2 \equiv \Delta m_{21}^2 = m_2^2 - m_1^2, \quad (4)$$

$$\Delta M^2 \equiv \Delta m_{31}^2 = m_3^2 - m_1^2. \quad (5)$$

The Δm^2 mass scale is taken to be of $\mathcal{O}(10^{-3})$ eV², as suggested by the Super-Kamiokande atmospheric data, while the ΔM^2 mass scale is taken to be of $\mathcal{O}(1)$ eV², as suggested by LSND. Furthermore, we shall only consider the case in which there is no CP-violation in the neutrino sector, and thus we shall set the phase $\delta = 0$.

3. The Super-Kamiokande Atmospheric Neutrino Data

Let us assume that at the top of the atmosphere, at $t = 0$, the number of muon and electron neutrinos produced are N_μ and N_e , respectively. Although both neutrinos and antineutrinos are produced in both flavors, we shall use the terms “muon neutrinos” and “electron neutrinos” loosely, to include both neutrinos and antineutrinos. The ratio of muon to electron neutrinos, r ,

$$r = \frac{N(\nu_\mu + \bar{\nu}_\mu)}{N(\nu_e + \bar{\nu}_e)} = \frac{N_\mu}{N_e} \quad (6)$$

is, in general, a monotonically increasing function of energy. However, for the relevant range of L/E values in Super-Kamiokande, r may be assumed constant ($r = 2$), as we shall do throughout this Letter. Within a detector at a distance $L \simeq t$ from the production point, the number of muon and electron neutrinos, N'_μ and N'_e , respectively, are given by:

$$N'_\mu = N_\mu P_{\mu\mu} + N_e P_{e\mu}, \quad (7)$$

$$N'_e = N_e P_{ee} + N_\mu P_{\mu e}, \quad (8)$$

where $P_{\mu\mu}$ is the ν_μ survival probability:

$$\begin{aligned} P_{\mu\mu} = & 1 - 4U_{\mu 1}^2 U_{\mu 2}^2 \sin^2 \left(1.27 \Delta m^2 \frac{L}{E} \right) - 4U_{\mu 1}^2 U_{\mu 3}^2 \sin^2 \left(1.27 \Delta M^2 \frac{L}{E} \right) \\ & - 4U_{\mu 2}^2 U_{\mu 3}^2 \sin^2 \left[1.27 (\Delta M^2 - \Delta m^2) \frac{L}{E} \right], \end{aligned} \quad (9)$$

$P_{e\mu}$ is the neutrino oscillation probability $P(\nu_e \rightarrow \nu_\mu)$:

$$\begin{aligned} P_{e\mu} = & -4U_{e1}U_{e2}U_{\mu 1}U_{\mu 2} \sin^2 \left(1.27 \Delta m^2 \frac{L}{E} \right) \\ & -4U_{e1}U_{e3}U_{\mu 1}U_{\mu 3} \sin^2 \left(1.27 \Delta M^2 \frac{L}{E} \right) \\ & -4U_{e2}U_{e3}U_{\mu 2}U_{\mu 3} \sin^2 \left[1.27 (\Delta M^2 - \Delta m^2) \frac{L}{E} \right], \end{aligned} \quad (10)$$

and P_{ee} is the ν_e survival probability:

$$P_{ee} = 1 - 4 U_{e1}^2 U_{e2}^2 \sin^2 \left(1.27 \Delta m^2 \frac{L}{E} \right) - 4 U_{e1}^2 U_{e3}^2 \sin^2 \left(1.27 \Delta M^2 \frac{L}{E} \right) - 4 U_{e2}^2 U_{e3}^2 \sin^2 \left[1.27 (\Delta M^2 - \Delta m^2) \frac{L}{E} \right]. \quad (11)$$

Since we are only considering the scenario with a vanishing CP-violating phase $\delta = 0$, $P_{\mu e} = P_{e\mu}$. The ratios of measured to predicted (without neutrino oscillations) μ -like and e -like events at Super-Kamiokande, R_μ and R_e , respectively, are

$$R_\mu = \frac{N'_\mu}{N_\mu} = P_{\mu\mu} + 0.5 P_{e\mu}, \quad (12)$$

$$R_e = \frac{N'_e}{N_e} = P_{ee} + 2.0 P_{\mu e}, \quad (13)$$

where we have explicitly set $r = 2$. It is precisely these two ratios, and in particular their L/E dependence - as measured by the Super-Kamiokande group - that we shall exploit in order to fully determine the neutrino oscillations mixing matrix.

For the mass scales considered here, something remarkable happens in the 3rd and in the 8th bin of the Super-Kamiokande atmospheric neutrino data - see Fig.4 in Ref.[9]. In the 3rd bin, corresponding to $10^{1.5} \text{ m/MeV} < L/E < 10^2 \text{ m/MeV}$, the oscillations involving the Δm^2 mass scale are approximately zero, and thus negligible, whereas the oscillations involving the ΔM^2 mass scale average out to $1/2$. One can certainly argue about how many oscillations it would take in a given L/E interval in order to safely assume that the oscillations do indeed average out. For instance, for $\Delta M^2 = 0.18 \text{ eV}^2$ one has approximately five oscillations in this interval, whereas $\Delta M^2 = 0.36 \text{ eV}^2$ yields obviously twice as many - approximately ten oscillations. In our view, even these relatively low numbers of oscillations do allow to effectively average out the sine squared variation. Therefore, we shall henceforth impose a weak lower bound of about 0.27 eV^2 for the ΔM^2 mass scale, as the average of the two values mentioned above. As we shall see later on, the value of ΔM^2 favored by this analysis lies well above this limit. In the 8th bin, corresponding to $10^4 \text{ m/MeV} < L/E < 10^{4.5} \text{ m/MeV}$, all oscillations average out to $1/2$. (For example, for $\Delta m^2 = 10^{-3} \text{ eV}^2$ one has approximately nine oscillations in this L/E interval, and thus our assumption is well justified.)

Following these arguments, the ratios of measured to expected μ -like and e -like events, as defined by Eqs.(12)–(13), are independent of the underlying mass scales in these two bins. For the 3rd bin, these ratios yield a rather simple form:

$$R_\mu^{(3)} = 1 - c_\beta^2 s_\psi^2 (2 - s_\beta^2 - 2c_\beta^2 s_\psi^2), \quad (14)$$

$$R_e^{(3)} = 1 - 2c_\beta^2 s_\beta^2 (1 - 2s_\psi^2). \quad (15)$$

They depend only on the 1-3 and 2-3 mixing angles, β and ψ , respectively. One could argue that using the values measured by Super-Kamiokande, $R_\mu^{(3)} = 0.908 \pm 0.068$

and $R_e^{(3)} = 1.225 \pm 0.108$, directly determine these two angles. However, at this point we prefer to only restrict the possible values of β and ψ from the ratio of ratios, $R_\mu^{(3)}/R_e^{(3)} = 0.741 \pm 0.088$. This is a much more robust quantity, as the large systematic errors in the individual flux calculations largely cancel out. The allowed values for the mixing angles β and ψ are shown in Fig. 1, at the $\pm 1\sigma$ level. The expressions for the μ -like and e -like event ratios in the 8th bin, $R_\mu^{(8)}$ and $R_e^{(8)}$, respectively, are rather long and cumbersome, and therefore we choose not to display them explicitly. With four data points (the ratios of ratios and the μ -like

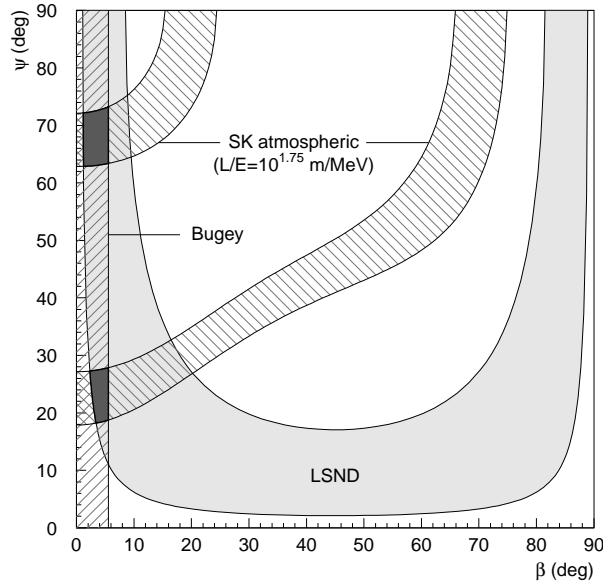


Fig. 1. Allowed regions for the mixing angles β and ψ from the Super-Kamiokande ratio of ratios in the 3rd L/E bin (see text), from the the LSND *appearance* signal (grey-shaded area), and from the Bugey *disappearance* measurement (hatched area left of $\beta = 5.5^\circ$).

ratios at the two bins) one can fit the three mixing angles, along with an overall flux normalization constant. This procedure determines the mixing angles to be $\theta = 8.3^\circ$, $\beta = 52.6^\circ$, and $\psi = 49.8^\circ$, for an overall scale factor of 0.88. The ratio of the measured to predicted solar neutrino flux, which is nothing else but the ν_e survival probability in Eq.(11) with all sine squared terms averaged to 1/2,

$$R_e^{Solar} = 1 - 2c_\beta^2(c_\theta^2 s_\theta^2 c_\beta^2 + s_\beta^2), \quad (16)$$

yields $R_e^{Solar} = 0.53$ for this particular set of angles. However, while this solution indicates a significant solar neutrino deficit, consistent with the current measurements, it is not compatible with other neutrino experiments, which we discuss in the following sections.

4. The LSND Experiment

The detector was located at 30 m from the neutrino source, with average neutrino energies of approximately 40 MeV and 110 MeV, for the decay-at-rest (DAR) and decay-in-flight (DIF) beams, respectively. We shall only consider the DAR results, as they are more restrictive and also more statistically significant than the DIF results. The $\bar{\nu}_\mu \rightarrow \bar{\nu}_e$ oscillation probability is given by Eq.(10). For $\Delta m^2 = \mathcal{O}(10^{-3})$ eV² the first sine squared term is negligible, while the remaining two can be combined by approximating $\Delta M^2 - \Delta m^2 \approx \Delta M^2$ to yield

$$P_{\mu e}^{LSND} = \sin^2(2\beta) \sin^2\psi \sin^2\left(1.27 \Delta M^2 \frac{L}{E}\right). \quad (17)$$

Comparing this with the two-generation neutrino oscillation expression

$$P_{\mu e}^{LSND} = \sin^2(2\Theta_{LSND}) \sin^2\left(1.27 \Delta M^2 \frac{L}{E}\right), \quad (18)$$

in terms of which the LSND event excess has been analyzed, one can effectively identify $\sin^2(2\Theta_{LSND})$ with $\sin^2(2\beta)\sin^2\psi$. The allowed regions obtained by this experiment from a preliminary analysis of the entire 1993-1998 DAR data¹⁸ is shown in Fig. 2(a). The excluded regions determined from the BNL-E776¹⁹ and KARMEN-2²⁰ experiments are also shown in the same figure. Considering these limits, we impose an upper bound for the ΔM^2 mass scale, $\Delta M^2 < 1.9$ eV², and a lower bound for the effective mixing, $\sin^2(2\beta)\sin^2\psi > 0.0014$. Furthermore, following the weak lower bound imposed by the oscillations averaging requirement, $\Delta M^2 > 0.27$ eV², implies an upper bound for the effective mixing, $\sin^2(2\beta)\sin^2\psi < 0.086$, as dictated by the boundary between the allowed region from LSND and the excluded region from BNL-E776. These limits determine the allowed region in the (β, ψ) mixing angles space illustrated by the grey-shaded area in Fig. 1. The recent KARMEN-2 limit would naturally impose a more stringent limit of $\sin^2(2\beta)\sin^2\psi < 0.051$. However, it turns out that the restrictions imposed by LSND on the angles β and ψ are rather weak as compared to the severe limits imposed by the Bugey reactor experiment, which we discuss in the next section.

5. The Reactor Experiments

The survival probability for electron (anti)neutrinos – as typically measured by all reactor experiments – is given by Eq.(11). The most restrictive reactor experiment for the relevant range of parameters considered in this paper is the Bugey experiment.²¹ It was carried out with three detectors at distances of 15 m, 40 m, and 95 m from the reactor core, with a mean neutrino energy of approximately 3 MeV. Following the same arguments as in the LSND discussion above, the first sine squared term in Eq.(11) is negligible, and the remaining two are combined to yield

$$P_{ee}^{Bugey} = 1 - \sin^2(2\beta) \sin^2\left(1.27 \Delta M^2 \frac{L}{E}\right). \quad (19)$$

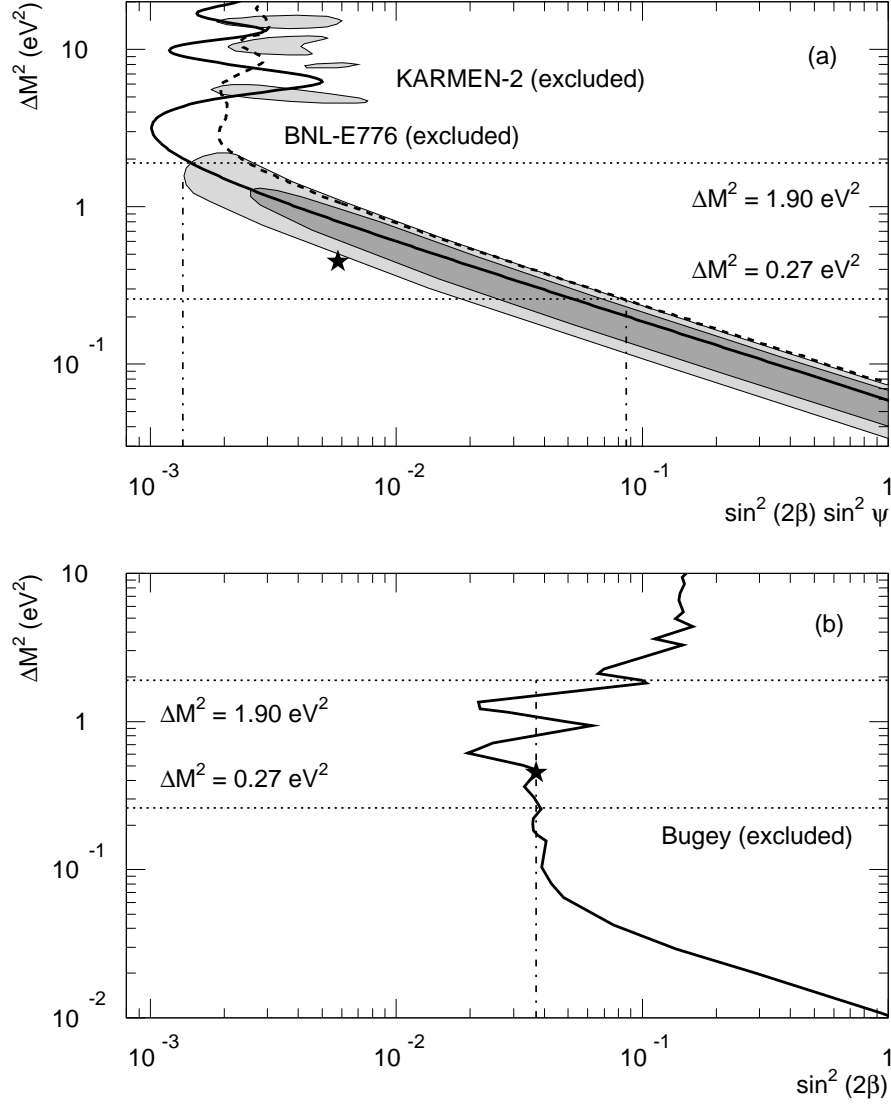


Fig. 2. (a) Allowed regions in the $(\sin^2(2\beta) \sin^2 \psi, \Delta M^2)$ space as obtained by the LSND DAR $\bar{\nu}_e$ appearance experiment (grey-shaded areas). The excluded regions obtained by the BNL-E776 and KARMEN-2 experiments are also shown (thick dashed and thick solid curves, respectively). The dot-dashed lines correspond to $\sin^2(2\beta) \sin^2 \psi = 0.0014$ and $\sin^2(2\beta) \sin^2 \psi = 0.086$. (b) Excluded region in the $(\sin^2(2\beta), \Delta M^2)$ space as obtained by the Bugey $\bar{\nu}_e$ disappearance reactor experiment. The dot-dashed line corresponds to $\sin^2(2\beta) = 0.037$. In both (a) and (b) the dotted lines correspond to the ΔM^2 limits considered here, while the point favored by this analysis is indicated by the dark star.

A direct comparison of Eq.(19) with Eq.(17) shows explicitly the difference between the disappearance and appearance probabilities in the three-generations neutrino oscillations formalism, as we have argued in the previous section. However, in this particular case, the expression given by Eq.(19) is fully equivalent with the ν_e disappearance probability that one would write in a two-generations mixing model,

$$P_{ee}^{Bugey} = 1 - \sin^2(2\Theta_{Bugey}) \sin^2\left(1.27 \Delta M^2 \frac{L}{E}\right). \quad (20)$$

Therefore, one can effectively identify $\sin^2(2\Theta_{Bugey})$ with $\sin^2(2\beta)$, or simply Θ_{Bugey} with β . Consequently, the same limits determined for Θ_{Bugey} apply to the mixing angle β in our formalism, as shown in Fig. 2(b).

Notice that the excluded region obtained by this experiment is not shown on the same figure with LSND, as one typically tends to do – see for example Refs.[18,20]. This is because LSND, BNL-E776, and KARMEN-2 are all appearance experiments, whereas Bugey is a disappearance one. In the two-generations neutrino oscillations formalism, plotting the excluded regions from a disappearance experiment on the same figure showing the excluded (or allowed) regions from an appearance experiment is perfectly legitimate. However, this is incorrect and misleading in the full three-generations mixing, where *appearance* and *disappearance* probabilities are characterized by different combinations of the mixing angles.

For the ΔM^2 mass scale discussed in this Letter, the Bugey reactor experiment severely restricts $\sin^2 2\Theta_{Bugey}$ to be < 0.037 , and herewith $\beta = \Theta_{Bugey} < 5.5^\circ$ – as indicated by the hatched area in Fig. 1 – at the 90% confidence level. This limit is obviously much more restrictive than the ones obtained from the LSND discussion above, limiting the mixing angles β and ψ to the two dark-shaded areas in Fig. 1. However, the relevance of the LSND result should not be underestimated. On one hand, it does not allow for β to become arbitrarily small, while on the other hand – and more importantly – it establishes the existence of the $\Delta M^2 = \mathcal{O}(1)$ eV² mass scale, which is crucial to our approach.

Before we go on and discuss the mixing matrix determined under these constraints, we would like to first discuss a general feature that emerges directly from the narrow intervals to which β and ψ are confined. Both areas of allowed values for β and ψ (the upper and lower dark-shaded areas in Fig. 1, henceforth referred to as A and B, respectively) are characterized by a very low mixing angle $\beta < 5.5^\circ$. This in turn implies that $s_\beta < 0.096$ and herewith, the expression for the ratio of measured to predicted solar neutrino flux given by Eq.(16) becomes

$$R_e^{Solar} = 1 - \frac{1}{2} \sin^2(2\theta) + \mathcal{O}(10^{-2}). \quad (21)$$

Consequently, a mixing angle θ of approximately 45° will automatically imply a solar neutrino ratio $R_e^{Solar} \simeq 0.5$. And this is actually exactly what happens. For values of β and ψ restricted to area B in Fig. 1, the angle θ must satisfy $20^\circ < \theta < 64^\circ$ for the predicted ratio of ratios in the 8th L/E bin, as a function of θ , to agree with the

value measured by Super-Kamiokande at the $\pm 1\sigma$ level, $R_\mu^{(8)}/R_e^{(8)} = 0.456 \pm 0.069$. (For mixing angles β and ψ in area A of Fig. 1 there is no θ solution at the $\pm 2\sigma$ level.) This implies that the solar neutrino ratio must be $0.49 < R_e^{Solar} < 0.78$. However, imposing a stricter agreement with the central value of $R_\mu^{(8)}/R_e^{(8)} = 0.456$, yields values of θ of approximately 35° and 50° , which in turn yield $R_e^{Solar} \simeq 0.56$ and $R_e^{Solar} \simeq 0.52$, respectively.

6. The Mixing Matrix and the LSND Mass Scale

Fitting the ratio of ratios and the μ -like event ratios at the two L/E bins, one obtains the following set of mixing angles: $\theta = 35.1^\circ$, $\beta = 5.5^\circ$, and $\psi = 23.3^\circ$, for an overall flux normalization factor of 0.87. Herewith, the mixing matrix reads explicitly

$$U = \begin{pmatrix} 0.815 & 0.572 & 0.097 \\ -0.559 & 0.730 & 0.394 \\ 0.155 & -0.375 & 0.914 \end{pmatrix}, \quad (22)$$

and the ratio of measured to expected solar neutrino flux is predicted to be $R_e^{Solar} = 0.55$. Notice that, instead of using the μ -like events, one may very well use the e -like events in determining the mixing angles. Despite the somewhat larger errors in the e -like event ratios, the result does not differ much from the previous one: $\theta = 32.5^\circ$, $\beta = 5.5^\circ$, $\psi = 24.6^\circ$, and thus $R_e^{Solar} = 0.58$.

For the mixing angles determined here, $\sin^2(2\Theta_{LSND}) = 0.0058$, and thus ΔM^2 is restricted to $0.5 \text{ eV}^2 < \Delta M^2 < 0.8 \text{ eV}^2$, as one can easily see from the LSND allowed region in Fig. 2(a), below the area excluded by KARMEN-2. Thus, the ΔM^2 mass scale range favored by this analysis is well above the weak limit of approximately 0.27 eV^2 imposed by the oscillations averaging argument. However, there is yet another mass limit that has to be considered at this point, namely as imposed by the CDHSW ν_μ disappearance experiment²² (illustrated in Fig. 3). This experiment was performed using a neutrino beam of approximately 2 GeV and two detectors at 130 m and 885 m from the mean neutrino production point. The ν_μ survival probability is given by Eq.(9), which becomes

$$P_{\mu\mu}^{CDHSW} = 1 - 4 \cos^2 \beta \sin^2 \psi (1 - \cos^2 \beta \sin^2 \psi) \sin^2 \left(1.27 \Delta M^2 \frac{L}{E} \right), \quad (23)$$

when neglecting the Δm^2 contribution, as discussed in the previous two sections. Comparing this with the two-generations probability

$$P_{\mu\mu}^{CDHSW} = 1 - \sin^2(2\Theta_{CDHSW}) \sin^2 \left(1.27 \Delta M^2 \frac{L}{E} \right), \quad (24)$$

and using the mixing angles obtained by this analysis ($\beta = 5.5^\circ$ and $\psi = 23.3^\circ$), one obtains $\sin^2(2\Theta_{CDHSW}) = 0.52$. For this value of the effective mixing, the values of ΔM^2 below 0.4 eV^2 are excluded at the 90% confidence level by this experiment. Therefore, we conclude that this mass scale must be restricted to $0.4 \text{ eV}^2 < \Delta M^2 <$

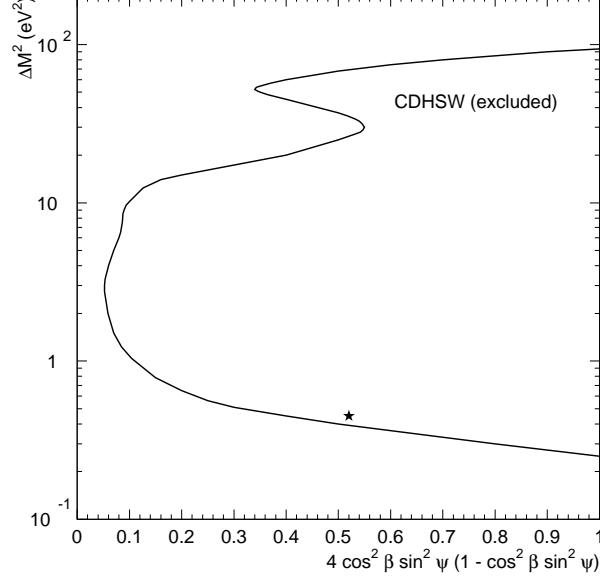


Fig. 3. Excluded region in the $(4 \cos^2 \beta \sin^2 \psi (1 - \cos^2 \beta \sin^2 \psi), \Delta M^2)$ space obtained by the CDHSW ν_μ disappearance experiment, along with the point favored by this analysis (dark star).

0.5 eV^2 , and we set it to $\Delta M^2 \simeq 0.45 \text{ eV}^2$ for the discussion below. With these parameters, the point favored by this analysis lies at the edge of the LSND allowed region and also at the edge of the Bugey and CDHSW excluded regions, as shown in Figs. 2(a), 2(b), and 3, respectively.

With the mixing matrix fully determined and with $\Delta m^2 = \mathcal{O}(10^{-3}) \text{ eV}^2$ and $\Delta M^2 \simeq 0.45 \text{ eV}^2$, we can also investigate the atmospheric neutrino ratio of ratios predicted by this analysis as compared to the Super-Kamiokande data. This is illustrated in Fig. 4(a) for $\Delta m^2 = 10^{-3} \text{ eV}^2$, as we shall make no attempt in this Letter to fit this mass scale. Our predicted μ -like and e -like event ratios are shown in Fig. 4(b), together with the Super-Kamiokande data rescaled by an overall factor of 0.87. In both cases the agreement between our prediction and the experimental data is reasonably good. No smearing of L/E has been included in our simulations.

7. Conclusions

We have shown that the L/E dependence of the Super-Kamiokande atmospheric neutrino data fully determines the three-generations neutrino mixing matrix, as given by Eq.(22). The only underlying assumption is that the mass scales involved are those determined by the atmospheric neutrino data, $\Delta m^2 = \mathcal{O}(10^{-3}) \text{ eV}^2$, and by the LSND experiment, $\Delta M^2 = \mathcal{O}(1) \text{ eV}^2$. Consequently, the ratio of measured to predicted solar neutrino flux is determined to be $R_e^{\text{Solar}} = 0.55$, independent

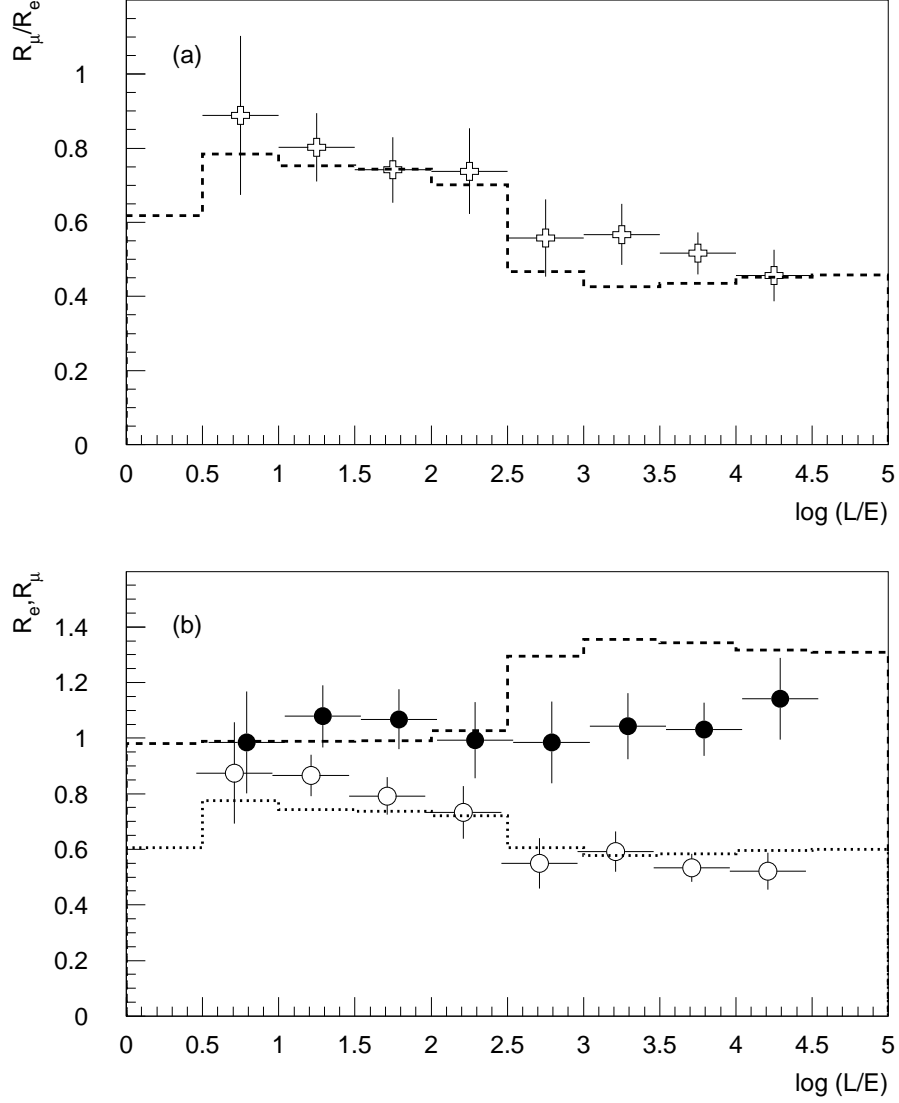


Fig. 4. (a) The predicted ratio of ratios (R_μ/R_e) versus $\log(L/E)$ – dashed histogram – compared to the Super-Kamiokande data (empty crosses with error bars). (b) The predicted μ -like (dotted) and e -like (dashed) event ratios (R_μ and R_e) versus $\log(L/E)$, compared to the Super-Kamiokande data (full and empty circles with error bars, respectively) scaled by a factor of 0.87. Both (a) and (b) have been obtained with $\Delta m^2 = 10^{-3} \text{ eV}^2$ and $\Delta M^2 = 0.45 \text{ eV}^2$.

of energy. While no attempt has been made here to determine a more precise value for Δm^2 , we believe that $\Delta M^2 \simeq 0.45 \text{ eV}^2$. This, together with the effective $\sin^2(2\Theta_{\text{LSND}}) = 0.0058$ determined here, lies just outside the sensitivity of the KARMEN-2 experiment, to be reached at the end of 2001. However, the Mini-BooNE experiment at FermiLab should see a significant number of $\nu_\mu \rightarrow \nu_e$ events at this mixing: approximately 345 (525) per year for $\Delta M^2 = 0.4$ (0.5) eV^2 . The long-baseline $\nu_\mu \rightarrow \nu_\tau$ appearance experiments (K2K, MINOS), which are probing the Δm^2 mass scale, should also see significant excess events for this particular neutrino mixing pattern. Higher statistics in the Super-Kamiokande atmospheric neutrino data and a more detailed analysis – which may include deviations of $r = N_\mu/N_e$ from the naive value of $r = 2$ due to geo-magnetic effects and L/E variations – should further restrict the mixing angles in this neutrino oscillations model, which involves the $\Delta m^2 = \mathcal{O}(10^{-3}) \text{ eV}^2$ and $\Delta M^2 = \mathcal{O}(1) \text{ eV}^2$ mass scales. However, should the LSND result prove to be wrong, it might be just as simple as: atmospheric deficit $\equiv \nu_\mu \rightarrow \nu_\tau$, and solar deficit $\equiv \nu_e \rightarrow \nu_x$. On the other hand, should the LSND result stand and should the solar neutrino deficit show a strong energy dependence, more complex neutrino models have to be invoked. Either way, if neutrino oscillations are firmly established, this will open exciting avenues beyond the physics of the Standard Model.

References

1. B. Pontecorvo, *Zh. Eksp. Teor. Fiz.* **33**, 549 (1957); *Sov. Phys. JETP* **6**, 429 (1958).
2. B. T. Cleveland *et al.*, *Nucl. Phys. B* **38** (Proc. Suppl.), 47 (1995).
3. Y. Fukuda *et al.*, *Phys. Rev. Lett.* **77**, 1683 (1996).
4. J. N. Abdurashitov *et al.*, *Phys. Lett. B* **328**, 234 (1994).
5. W. Hampel *et al.*, *Phys. Lett. B* **388**, 364 (1996).
6. Y. Fukuda *et al.* (Super-Kamiokande Collaboration), hep-ex/9812011.
7. K. S. Hirata *et al.*, *Phys. Lett. B* **280**, 146 (1992).
8. R. Becker-Szendy *et al.*, *Phys. Rev. D* **46**, 3720 (1992).
9. Y. Fukuda *et al.* (Super-Kamiokande Collaboration), *Phys. Rev. Lett.* **81**, 1562 (1998).
10. C. Athanassopoulos *et al.* (LSND Collaboration), *Phys. Rev. C* **54**, 2685 (1996).
11. C. Athanassopoulos *et al.* (LSND Collaboration), *Phys. Rev. C* **58**, 2489 (1998).
12. R. P. Thun and S. McKee, *Phys. Lett. B* **439**, 123 (1998).
13. G. Barenboim and F. Scheck, *Phys. Lett. B* **440**, 332 (1998).
14. T. Teshima and T. Sakai, hep-ph/9805386, hep-ph/9901219.
15. T. Ohlsson and H. Snellman, hep-ph/9903252.
16. L. Maiani, *Phys. Lett. B* **62**, 183 (1976).
17. D. V. Ahluwalia and T. Goldman, *Phys. Rev. D* **56**, 1698 (1997).
18. R. Tayloe, talk presented at the *Lake Louise Winter Institute*, Lake Louise, Canada, 14-20 February, 1999.
19. L. Borodovsky *et al.*, *Phys. Rev. Lett.* **68**, 274 (1992).
20. K. Eitel, talk presented at the *Lake Louise Winter Institute*, Lake Louise, Canada, 14-20 February, 1999.
21. B. Achkar *et al.*, *Nucl. Phys. B* **434**, 503 (1995).
22. F. Dydak *et al.*, *Phys. Lett. B* **134**, 281 (1984).